Aalto University

Fearon, Olesya; Nykänen, Vesa; Kuitunen, Susanna; Ruuttunen, Kyösti; Alén, Raimo; Alopaeus, Ville; Vuorinen, Tapani

Detailed modeling of the kraft pulping chemistry : carbohydrate reactions

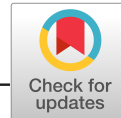# Detailed modeling of the kraft pulping chemistry: carbohydrate reactions

Olesya Fearon[1] [ID] | Vesa Nykänen[2] | Susanna Kuitunen[3] | Kyösti Ruuttunen[1] |
Raimo Alén[2] | Ville Alopaeus[4] | Tapani Vuorinen[1]

[1]Department of Bioproducts and Biosystems, Aalto University, School of Chemical Engineering, Aalto, Finland

[2]Laboratory of Applied Chemistry, University of Jyväskylä, Jyväskylä, Finland

[3]Neste Engineering Solutions Oy, Porvoo, Finland

[4]Department of Chemical and Metallurgical Engineering, Aalto University, School of Chemical Engineering, Aalto, Finland

Correspondence
Olesya Fearon, Aalto University, P.O. Box 16300, 00076 Aalto, Finland.
Email: olesya.fearon@aalto.fi

Abstract

The article introduces a detailed model for carbohydrate chemistry in kraft pulping. This article is continuation to the modeling work carried out for hot water extraction and chemical pulp bleaching. The model includes galactoglucomannan, xylan, and cellulose acid–base equilibria, in addition to peeling, stopping, and alkaline hydrolysis reactions of the same carbohydrates, as well as hexenuronic acid formation and degradation reactions. The Arrhenius parameters were applied from the literature or regressed against experimental data in the present study. The model is very successful in predicting the experimental data of carbohydrate reactions during kraft pulping. Many features of the pulping-related model can be applied to specific fractionation chemistry considerations. The detailed knowledge on carbohydrates composition at any stage of pulping gives possibility for further development of biorefinery cases based on kraft pulping, such as biofuel and chemicals production.

KEYWORDS

carbohydrates, kraft pulping, modeling, reaction kinetics, reaction mechanism

1 | INTRODUCTION

Currently, the kraft pulping process is globally the most common pulping process. The popularity of this process can be explained by high strength properties of the pulp, relatively easy recovery of the cooking chemicals and the use of dissolved organic material for energy production.[1] On the other hand, disadvantages of kraft pulping process include the dark color of unbleached pulp, the loss of pulp yield due to carbohydrate degradation and solubilization, as well as the formation of odor compounds.[1] The main cooking chemicals in kraft pulping are sodium hydroxide and sodium sulfide in a highly alkaline aqueous solution, called white liquor. During delignification, the white liquor interacts with the wood, resulting in the formation of black liquor, which is a complex mixture of degraded lignin, carbohydrates, carboxylic acids, extractives and chemicals.[2]

The carbohydrate yield loss in kraft pulping, due to degradation and dissolution of polysaccharides, is substantial and a serious drawback of the process.[1] In kraft pulping, the significant consumption of alkali takes place due to the rapid hydrolysis of acetyl groups in hemicelluloses (i.e., galactoglucomannan in softwoods and xylan in hardwoods)[3] and peeling reactions of wood polysaccharides, where sugar units are lost one-by-one from the reducing end of the polysaccharide (primary peeling). During the heating period of pulping, new reducing end groups are forming enabling secondary peeling. The peeling reactions are interrupted by competing stopping reactions, which convert the reducing end groups into stable carboxylic acid groups.[2] Both softwood and hardwood xylans contain 4-O-methyl glucuronic acid (MeGlcA) side groups. In alkaline conditions MeGlcA are converted into hexenuronic acid (HexA) groups by elimination of methanol.[4] However, these acid groups attached to the xylan backbone are

relatively stable under alkaline conditions and contribute substantially to the total amount of acidic groups in kraft pulps.[5] Cellulose is a more resistant carbohydrate component against alkali in comparison with hemicelluloses, which degrade much more extensively. The overall carbohydrate degradation reactions in kraft pulping are presented in Figure 1.

In order to obtain a better understanding of alkali pulping processes, the reaction kinetics of carbohydrates and lignin degradation have been studied over the years. Different models have been developed for kraft pulping process. The first model was presented by Vroom.[6] Kleinert[7] studied lignin and carbohydrate reaction kinetics as a function of temperature and alkali charge. Later, Hatton[8] implement a model that predicts the kappa number and residual lignin content, based on H-factor and effective alkali (EA) charge. LeMon and Teder[9] were the first who presented the "3-stage model" approach to the scientific community. Another type of model is Purdue model[10] where wood chips are divided to several components: cellulose, galactoglucomannan, xylan and lignin (high and low reactivity). Later, Purdue model was extended by Christensen,[11] where dependence of reactivity on hydroxide and hydrogen sulfide ions was added. Gustafson[12] developed a 3-stage model based on differential pulping periods. In 3-stage model, degradation of carbohydrates depends on the delignification rate in each phase. Later, the model was improved by modeling individually cellulose and hemicellulose degradation.[13] Another model, presented by Gustafson and Al-Dajani[14] was based on carbohydrates as individual species (cellulose, galactoglucomannan, and xylan) and could be described by the first order reaction. Additionally, the effect of hydroxide and hydrogen sulfide ions is included in the model. New attempt to improve Purdue model was done by Andersson et al.[15] In work,[15] degradation of all wood components is demonstrated by individual parallel equations, in total—12 pseudocomponents. However, the model parameters do not

distinguish different carbohydrate species. The model represented by Johansson[16] is based on the idea how alkali and sodium concentration affect carbohydrates' behavior in kraft pulping. However, the model was based on experimental data from later stage of pulping, and consequently initial dissolution and primary peeling of carbohydrates could not be included. Therefore, this model was focused on alkaline hydrolysis instead of whole kraft pulping process.

Wigell[17] described glucomannan degradation in alkaline pulping by power law equation. Galactoglucomannan was described by the amount of insoluble material, degradation through alkaline hydrolysis and primary peeling. Later, Nieminen[18] presented a mathematical model where primary and secondary peeling, as well as stopping and alkaline hydrolysis reactions were included. Wigell[17] described xylan and galactoglucomannan degradation similarly in their model; however, this is not acceptable: galactoglucomannan degrades as a result of endwise degradation through primary and secondary peeling following alkaline hydrolysis, whereas xylan degradation due to endwise peeling is limited.[19,20] Components such as arabinose and glucuronic acid presented on the backbone of the xylan polysaccharide stabilize its structure.[21] Additionally, degradation products of xylan are polymers, Dissolution of xylan polymers is dependent on the porosity of cell wall.[22] After degradation of lignin and other hemicelluloses, porosity of cell wall increases and improves the dissolution of xylan.[22] Therefore, xylan degradation cannot be modeled in the same way as galactoglucomannan, which means that a more complex scheme for degradation and dissolution of xylan has to be developed. Another model dealing with kraft pulping is model by Bogren et al.[23] The model includes time-dependent rate constant and mathematical pre-exponent that are dependent on the degree of delignification and temperature. However, the model is challenging to use due to many adjustable "parameters." For example, in order to predict xylan removal in kraft pulping, 10 parameters are required. In general, the
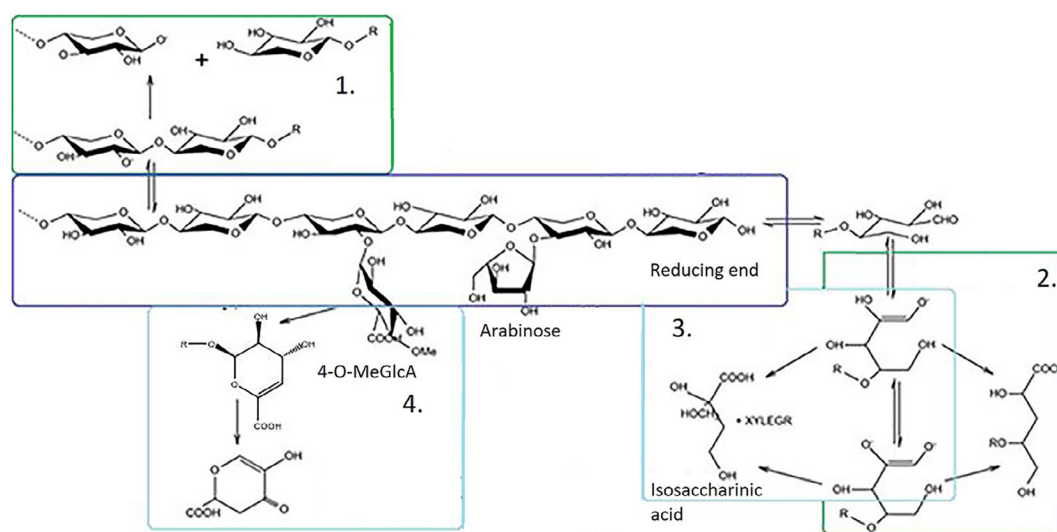
FIGURE 1   Carbohydrate reactions in kraft pulping, where *R* is a carbohydrate chain. (1) Alkali-catalyzed hydrolysis; (2) stopping reactions of reducing end groups; (3) alkali-catalyzed peeling of reducing end groups; (4) formation and degradation of hexuronic acid groups (HexA) [Color figure can be viewed at wileyonlinelibrary.com]

problem for most of empirical models is that they are based on adjusting mathematical simulation results to experimental data.

Wishnewski[24] developed a continuous digester model (extended Purdue model) based on Purdue model. They implemented a lumped-parameter approximation, used to describe the flow transport mechanism. As a result, a model based on the fundamental principles of mass and energy was developed. In that model, fewer simplifying assumptions in the model derivation are needed, because of definition of mass bases and volume fractions. Further Bhartiya[25] presented a model where digester thermal–hydraulic model was combined with Purdue model. The benefits of hydraulic extension were presented by the ability of the model to explain the impact of dynamic flow rate and compaction changes on pulp quality. Additionally, the model was able to explain operation difficulties taking place during hardwood to softwood transition. Another simulation-cooking model (Lo-Solids™) is a developed by Miyanishi and Shimada.[26] The model is a steady-state simulation of continuous cooking systems. The kinetic model utilized in the simulation is based on Purdue model.[10,11] The model includes, besides earlier presented components (high and slow reactive lignin, cellulose, galactoglucomannan, and xylan), also extractives.[26] They are assumed to dissolve extremely fast already in the beginning of cooking. The degradation of the other five components is modeled based on initial, bulk and residual phases of cooking. Additionally, the model is divided into three phases: wood components, as well as entrapped and free liquor.[26] Choi and Kwon[27,28] have developed a complex model that is able to regulate Kappa number, porosity evolution and cell wall thickness of wood chips. The model includes Purdue model for delignification of wood chips, kinetic Monte-Carlo algorithm to describe the evolution of micro configuration and model-based feedback control system to regulate kappa number, cell wall thickness and/or porosity simultaneously.[27,28] Those parameters are important for future studies of microscopic properties and their effect on paper properties.

Looking into all mentioned models above, it is clear that they are not taking into the consideration all chemical phenomena. By contrast, our aim is to create in-depth knowledge on the existing and possible new cooking processes. Model, presented in this work based on simulation of individual reactions and combining them together for an overall phenomenon. This is especially crucial for the development a biorefinery cases, where understanding chemistry of each wood fraction is necessary. Additionally, in order to improve prediction of the models, the amount of assumptions has to be limited. A general model with empirical kinetic equations may give a good fitting for individual cases; however, they rarely can give reliable prediction results for a wide range of experimental setups due to the fact that the equations, most often, have no physical or chemical meaning and they are just representing mathematical fitting.

In this work, the main aim is to create a detailed method for simulating chemical and physical phenomena in kraft pulping. The concept of two liquid phases was applied to take into account the ion distribution (Donnan effect)[29] and to separate the effect of mass transfer and reaction kinetics. The amount of hemicellulose reactions depends on the desired outcome. When producing dissolving pulp, the

hemicelluloses should be removed almost completely (in addition to removing lignin).[51] However, when producing paper grade pulp, it is beneficial to have a relatively high hemicellulose content, because that improves the binding of the cellulosic fibers with each other in the paper.[1] During pulping (also in the case of paper grade pulp) limited removal of hemicelluloses is beneficial for better mass transfer: for example, the lignin molecules can leach out more easily from the cell wall structure, when it becomes more porous, that is, some hemicelluloses are degraded and dissolved. The present model, taking advantage of fundamental understanding of the identified reactions and can be applied to optimize the pulp production process. The current paper focuses on hemicellulose reactions in kraft pulping and Fearon et al[30] paper focuses on delignification model in kraft pulping.

2 | MODEL

In the present paper, carbohydrate reaction model in kraft pulping conditions is discussed. In our other recent work,[30] the general idea of the model and the details of modeling lignin reactions were presented.

Pine wood composition used in the model development was approximated by utilizing literature data from similar types of wood[2,31,32] (Table 1). The initial composition of pulping liquor as well as such parameters as temperature, pressure, and liquid-to-wood ratio, were varied depending on the experimental setup. Extremely fast mass transfer was assumed, by the fact that experimental studies with wood meal[31-33] were utilized for the model validation and parameter optimization. Parameter regression with Kinfit software[34] using Levenberg–Marquardt optimization algorithm was used to obtain the unknown model parameters.

The model follows time evolution of compounds presented in Table 1 during pulping as well as formation of new compounds. The contents of Ca^{2+} and uronic acids determine the magnitude of the Donnan effect in the model.

This paper is organized so that the modeled degradation of each type of carbohydrate polymer—galactoglucomannan(GGM), xylan (XYL), and cellulose—is presented separately. A list of chemical reactions and reaction parameters is presented in Tables 2–4.

3 | RESULTS AND DISCUSSION

Carbohydrate and lignin parameters were regressed separately, therefore carbohydrate parameters could be underestimated because of yield loss due to lignin removal and increasing fiber saturation point (FSP) were not included in the simulations. FSP is a measure of the amount of water bound to the fiber wall.[35]

3.1 | Modeling of galactoglucomannan reactions

Native GGM polymers were modeled as a set of three types of units: reducing end group (GGMR), nonreducing end group (GGMNR), and

TABLE 1 Composition of Scots pine (*Pinus sylvestris* L.)[2,31,32] used for simulations

Component	Content	
	(%)	(mol/kg)
Lignin	26.8	
Nonphenolic (etherified) guaiacyl		1.07
Guaiacyl phenol		0.32
Nonphenolic guaiacyl with carbonyl group in α carbon		0.0081
Cellulose	41.8	
Group in the middle of the cellulose chain		2.466535
Reducing end group of cellulose chain		0.000245
Nonreducing end group of cellulose chain		0.000223
Glucomannnan	16.9	
Glucomannan group in the middle of the chain		1.02
Reducing end group in glucomannan		0.0102
Nonreducing end group in glucomannan		0.0102
Arabinoxylan	8.4	
Group in the middle of the xylan chain		0.5784
Reducing end group of xylan chain		0.0056
Nonreducing end group of xylan chain		0.0056
4-O-methyl-D-glucuronic acid		0.08
Other carbohydrates	1.5	
Arabinogalactan galactose nonreducing end-group		0.0106
Arabinogalactan middle group		0.0160
Arabinogalactan arabinose nonreducing end group		0.0071
Methyl esterified galacturonan middle group		0.2308
Galacturonan middle group (non-esterified)		0.1539
Arabinose structure in hemicellulose		0.00056
Extractives	3.4	
Ca		0.00021
K		0.00029
Mg		0.00007

units in the middle of the chain (GGMM). One end of the GGM polymer was assumed to be reducing and the other one nonreducing. The degree of polymerization of GGM in wood was assumed to be 102.[2]

In alkaline conditions, the reducing end groups and the middle units of GGM undergo reversible acid–base equilibrium reactions that were added to the model (Table 2, GE1–GE3). The pK$_a$ values for GE1 and GE2 were fitted in Kinfit software based on the work of Paananen.[32] For comparison, pK$_a$ values of 10.89 and 12.49 were reported in literature.[36] The pK$_a$ value for GE3 was compared with the pK$_a$ value of 14.28 reported for cellulose.[37] The ionization heat of glucose and mannose were reported to be 36.7 and 33.1 kJ/mol, respectively.[38] The ionized reducing end groups undergo the peeling or stopping reactions (G1–G3).[39] Activation energy for galactoglucomannan peeling reaction (G1 and G2) has been reported to be 84.6 kJ/mol.[39] The alkaline hydrolysis reaction (G4) can be encountered by intramolecular bond cleavage in the ionized middle units.[40]

However, the scheme described above did not give satisfactory results in fitting between experimental and simulated results. Improvements to the model were achieved by addition of a new stopping reaction (G5) that describes the possibility of the formation of metasaccharinic acid even at low alkali concentrations. The match between experimental and modeled data were significantly improved after this addition. In Tables 2–4 in reaction stoichiometry, bolded reaction species were in rate equations. Reported in literature values[36-39] were very close to the values obtained from regression in Kinfit (Table 2).

Simulation results of GGM degradation and dissolution are presented in Figure 2. The experimental data from Paananen[32] was used for the model validation. Parameters for GGM degradation were obtained from the fitting and then alkali-catalyzed deacetylation and cleavage of uronic acids esters were included to the model. The model accurately fitted the experimental data.

3.2 | Modeling of xylan reactions

The XYL degradation reaction routes are very similar to those with GGM. The units considered in the model were reducing end-group units (XYLR), nonreducing end group units (XYLNR), and units in the middle group in the xylan chain (XYLM). Additionally, it was assumed that arabino(4-O-methylglucurono)xylan has two kinds of side-groups. Of them, 4-O-methylglucuronic acid (MeGlc) side-groups were treated as individual compounds, whereas arabinose side groups were considered as leaving groups that enhance the conversion of a reducing end group in xylan into a stable metasaccharinic acid group through the stopping reaction. During pulping, a considerable amount of xylan is also dissolved as polymer and this feature was included in the model. The degree of polymerization for xylan was assumed to be 106.[2] Initially, one end was assumed to be reducing and the other end nonreducing.

As it was mentioned, XYL was modeled in the same way as GGM to encounter peeling (Table 3; X1 and X2), stopping (X3 and X4) and alkaline hydrolysis (X5) as well as reversible acid–base equilibrium reactions which were included in the model (Table 3; XE1-XE3). All kinetic parameters presented in Table 3 were regressed in Kinfit software based on Paananen[32] data. Comparison values from Chen[41] were used to prove the fitting results, of 11.69 and 12.59 for XE1 and XE2, respectively. In addition, the value for XE3 could be compared to the value of 14.28 reported for cellulose.[37] A proton ionization heat, reported by Christensen,[38] of 37.7 kJ/mol for xylose was used in the model. The formation of arabinose during peeling (X1 and X2) and alkaline hydrolysis (X5) represent the fact that, in average, every 10th xylan middle unit has an arabinose side-group.[2] The formation of

TABLE 2 Parameters for GGM degradation scheme obtained from fitting in Kinfit. SSE 5.49×10^{-3}

R	Reaction stoichiometry	pK$_a$ (25°C)	$\Delta H_{f,reaction}$ (kJ/mol)	
GE1	GGMR(f) ↔ GGMR(−f) + H$^+$	10.7 ± 1.4	−(33.5 ± 8.4)	
GE2	GGMR(−f) ↔ GGMR(−2f) + H$^+$	11.7 ± 3.6	−(34.3 ± 13.0)	
GE3	GGMM(f) ↔ GGMM(−f) + H$^+$	14.6 ± 15.0	−(8.8 ± 2.1)	

	Reaction stoichiometry	A (s^{-1})	k (25°C/s)	Ea (kJ/mol)
G1	GGMM(f) + **GGMR(−f)** → GGMR(f) + Isosaccharinic acid (−aq)	1.97×10^9	$(1.20 \pm 0.71) \times 10^{-5}$	81 ± 4
G2	GGMM(f) + **GGMR(−2f)** → GGMR(−f) + Isosaccharinic acid (−aq)	1.92×10^{13}	$(8.58 \pm 1.45) \times 10^{-5}$	105 ± 12
G3	**GGMR(−2f)** → Metasaccharinic acid (−f) + HO$^-$	1.82×10^{12}	$(3.07 \pm 1.45) \times 10^{-7}$	107 ± 7.8
G4	**GGMM(−f)** + GGMM(f) + H$_2$O(aq) → GGMR(−f) + GGMNR(f)	2.79×10^{13}	$(2.53 \pm 0.84) \times 10^{-11}$	137 ± 14
G5	**GGMR(−f)** → Metasaccharinic acid(−f) + HO$^-$	1.97×10^{10}	$(5.70 \pm 5.34) \times 10^{-9}$	106 ± 12

TABLE 3 Parameters for xylan degradation and dissolution, scheme obtained from fitting in Kinfit. SSE 5.93×10^{-2}

R	Reaction stoichiometry	pK$_a$ (25°C)	$\Delta H_{f,reaction}$ (kJ/mol)
XE1	XYLR(f) ↔ XYLR(−f) + H+	11.8 ± 8.9	−(24.0 ± 7.2)
XE2	XYLR(−f) ↔ XYLR(−2f) + H+	12.6 ± 4.7	−(42.4 ± 14.3)
XE3	XYLM(f) ↔ XYLM(−f) + H+	14.4 ± 6.2	−(6.3 ± 2.4)

R	Reaction stoichiometry	A (s^{-1})	k (25°C/s)	Ea (kJ/mol)
X1	1.1 XYLM(f) + **XYLR(−f)** → XYLR(f) + XyloIsoSaccA[a](−aq) + 0.1 arabinose(f)	8.3×10^{12}	$(5.2 \pm 0.8) \times 10^{-6}$	104 ± 4
X2	1.1 XYLM(f) + **XYLR(−2f)** → XYLR(−f) + XyloIsoSaccA (−aq) + 0.1 arabinose(f)	6.0×10^{10}	$(3.4 \pm 0.3) \times 10^{-5}$	87 ± 11
X3	**XYLMR(−f)** + arabinose(f) + H$_2$O(aq) → XyloMetaSaccA (−f) + arabinose(aq)	1.3×10^9	$(8.4 \pm 2.1) \times 10^{-7}$	87 ± 7
X4	**XYLMR(−2f)** → XyloMetaSaccA[b](−f) + HO$^-$	3.6×10^{12}	$(4.9 \pm 0.2) \times 10^{-7}$	108 ± 7
X5	**XYLM(−f)** + 1.1 XYLM(f) + H$_2$O(aq) → XYLR(−f) + XYLNR(f) + 0.1 arabinose(f)	1.4×10^{13}	$(8.5 \pm 0.8) \times 10^{-11}$	132 ± 13
X6	**XYLM(f)** + OH(−aq) → XYLM(aq) + OH(−aq)	6.0×10^{14}	$(7.6 \pm 1.2) \times 10^{-13}$	154 ± 4
X7	**MeGlc(−f)** + HO$^-$ → HexA(−f) + methanol(aq) + HO$^-$	7.38×10^{11}		122
X8	**HexA(−f)** + HO$^-$ → COMA(−aq) + HO$^-$	8.05×10^{11}		126

[a]XyloIsoSaccA, xyloisosaccharinic acid.
[b]XyloMetaSaccA, xylometasaccharinic acid.

xylometasaccharinic acid (X3) takes place when an arabinose unit is in the reducing end unit. Equal dissolution rate was assumed for all XYL polymers. The dissolved XYL was assumed to be degraded at the same rate as the fiber-bound XYL. Possible readsorption of dissolved XYL, on the pulp surface, was not considered.

Simulation results of degradation and dissolution of XYL are presented in Figure 3. Experimental data from Paananen[32] were used for model parameter regression. The predicted XYL degradation shows a good correlation with the experimental data.

4-Deoxy-4-hexenuronic acid (HexA) is formed from MeGlc.[42] According to Johansson et al,[42] HexA degrades to 4-oxo-4*H*-pyran-2-carboxylic acid (comanic acid, COMA).[14] In alkaline conditions, both these uronic acids are in dissociated form (their pK$_a$ values are about 3)[43] contributing to the ion exchange (the Donnan effect). The

reaction kinetic parameters for HexA simulation (X7 and X8) were obtained from Bogren's[44] work. All other parameters for simulations were fitted with Kinfit software.[34]

HexA profiles were modeled by utilizing Bogren's experimental data[44] and Bogren's model.[23,45] The model presented in this article has a better fit to Bogren's experimental data then their own model, as could be seen in Figure 4a. The Bogren's model output deviated from the Bogren's experimental data[44] in the way as it deviated from our developed model output. The possible reason is in the Donnan effect. The current model took into consideration the decreasing Donnan effect as HexA is cleaved from the fiber wall, whereas in the Bogren's model the Donnan effect was assumed to be constant through the simulations. Nieminen and Kuitunen have discussed importance of Donnan effect on simulation results.[29,46]

TABLE 4 Parameters for cellulose degradation scheme obtained from fitting in Kinfit. SSE 5.54×10^{-3}

R	Reaction stoichiometry	pK$_a$ (25°C)		$\Delta H_{f,reaction}$ (kJ/mol)
CE1	CR(f) ↔ CR(−f) + H$^+$	11.5 ± 7.2		−(37.1 ± 11.7)
CE2	CR(−f) ↔ CR(−2f) + H$^+$	12.2 ± 4.9		−(40.7 ± 11.8)
CE3	CM(f) ↔ CM(−f) + H$^+$	14.7 ± 5.4		−(1.5 ± 0.6)
R	Reaction stoichiometry	A (s^{-1})	k (25°C/s)	Ea (kJ/mol)
C1	CM(f) + **CR(−f)** → CR(f) + Isosacch[a] (−aq)	3.55×10^{13}	$(2.68 \pm 1.18) \times 10^{-6}$	109.1 ± 7.4
C2	CM(f) + **CR(−2f)** → CR(−f) + Isosacch (−aq)	2.40×10^{13}	$(2.76 \pm 2.08) \times 10^{-4}$	96.7 ± 5.6
C3	**CR(−2f)** → Metasacch[b] (−f) + HO$^-$	3.59×10^{14}	$(3.13 \pm 1.26) \times 10^{-8}$	125.1 ± 11.3
C4	**CM(−f)** + CM(f) + H$_2$O(aq) → CR(−f) + CNR(f)	8.25×10^{13}	$(1.07 \pm 0.89) \times 10^{-13}$	153.5 ± 20.7

[a]Isosacch, isosaccharinic acid.
[b]Metasacch, metasaccharinic acid.
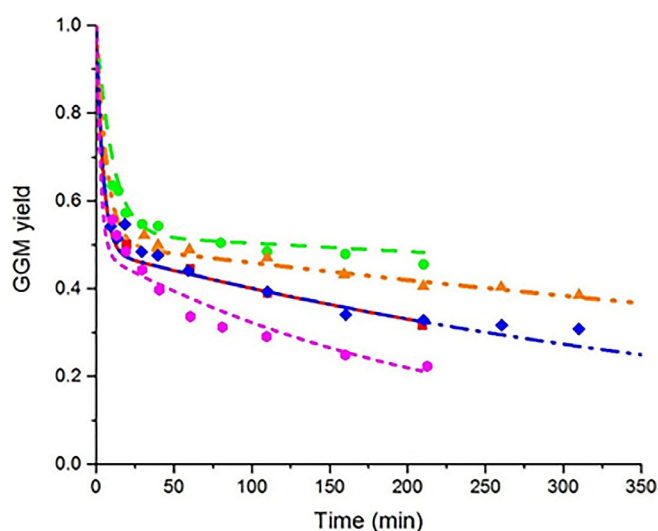
FIGURE 2 Galactoglucomannan degradation at [HO$^-$] = 1.55 M, [HS$^-$] = 0.31 M. Experimental data points[32] represented by symbols, simulation results expressed by lines. ■, —: 150°C, [Cl$^-$] = 0 M; ●, – – – –: 130°C, [Cl$^-$] = 0.14 M; ▲, - .. - .. -: 140°C, [Cl$^-$] = 0.14 M; ♦, - . - . -: 150°C, [Cl$^-$] = 0.14 M; ●, - - - -: 160°C, [Cl$^-$] = 0.14 M [Color figure can be viewed at wileyonlinelibrary.com]
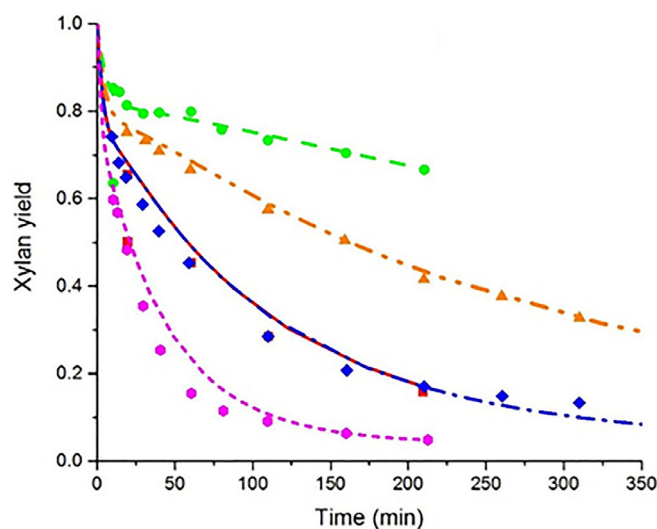
FIGURE 3 Xylan degradation at [HO$^-$] = 1.55 M, [HS$^-$] = 0.31 M. Experimental data points[32] represented by symbols, simulation results expressed by lines. ■, —: 150°C, [Cl$^-$] = 0 M; ●, – – – –: 130°C, [Cl$^-$] = 0.14 M; ▲, - .. - .. -: 140°C, [Cl$^-$] = 0.14 M; ♦, - . - . -: 150°C, [Cl$^-$] = 0.14 M; ●, - - - -: 160°C, [Cl$^-$] = 0.14 M [Color figure can be viewed at wileyonlinelibrary.com]

In Figure 4a effect of temperature on HexA formation and degradation is clearly shown. HexA degradation took place at temperatures higher than 139°C and proceeded faster at higher temperatures. Figure 4b represents how alkali concentration affects the amount of HexA. As shown on the Figure 4b—when [HO$^-$] is low (0.25 mol/kg) HexA formation is slow and degradation is insignificant, with higher alkali (0.51 mol/kg) HexA is formed and degraded, and at higher alkali (0.77 mol/kg) HexA is rapidly formed and degraded. The prediction is in line with the experimental values and showed that at higher alkalinities a competing formation and degradation of HexA proceeds faster than at lower alkali concentrations. This result is in line with earlier research[47] where it is shown that the rate of HexA formation in pulp, as well as its decomposition, is a function of hydroxide ion concentration.

3.3 | Modeling of cellulose reactions

Native cellulose polymers were modeled to consist of reducing end-group units (CR), nonreducing end group units (CNR) and the units in the middle of the chain (CM). The degree of polymerization of cellulose wood was assumed to be equal to 10,000.[2] Cellulose degradation was modeled using the previous scheme including: reversible acid–base equilibrium, peeling, stopping and alkaline hydrolysis reactions. Reversible acid–base equilibrium reactions for cellulose are presented in Table 3(CE1–CE3). For the alkaline hydrolysis, a pK$_a$ value of 14.28 has been published for cellulose.[37] Activation energy for peeling reaction has been reported to be 100.3 kJ/mol for cotton hydrocellulose[48] and 101 kJ/mol for cellulose.[49] The published activation energy for the stopping reaction are 134.8 kJ/mol and 100 kJ/mol for cotton
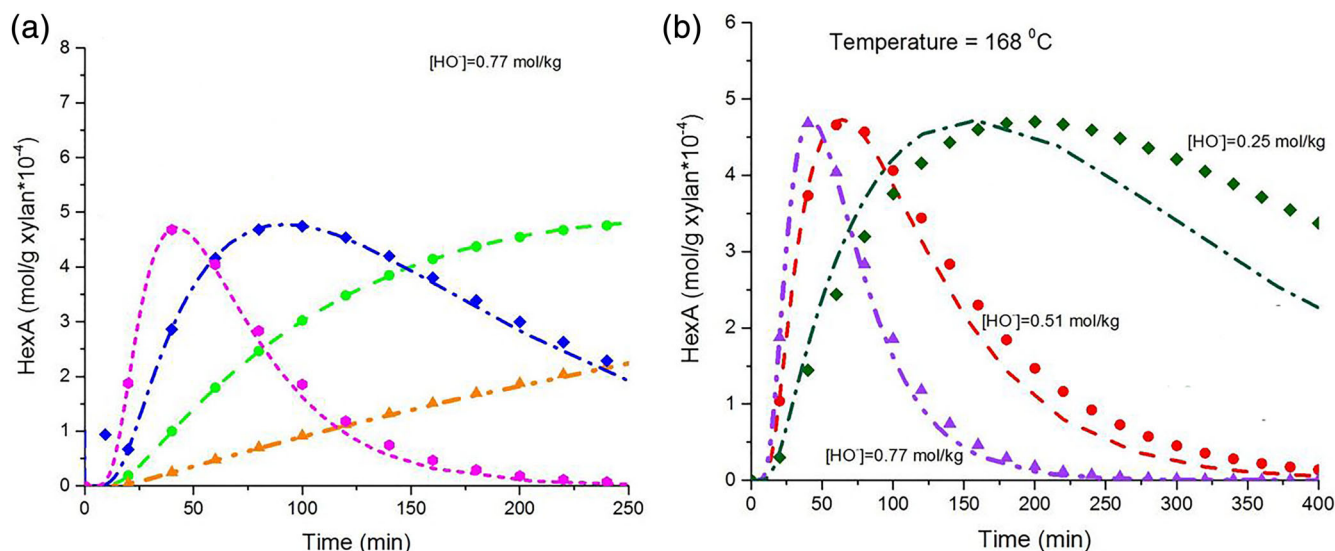
FIGURE 4 HexA formation and degradation. Experimental data points[44] represented by symbols, simulation results expressed by lines. (a) Effect of temperature on HexA at [HO⁻] = 0.77 mol/kg: ●, - - - -: 139°C; ▲, - . - . -: 123°C; ♦, -- . -- . --: 154°C; ●, -----: 168°C. (b) Effect of alkali concentration on the amount of HexA at 168°C: ●, - - - -: [HO⁻] = 0.51 mol/kg; ▲, - .. - .. -: [HO⁻] = 0.77 mol/kg; ♦, - . - . -: [HO⁻] = 0.25 mol/kg [Color figure can be viewed at wileyonlinelibrary.com]
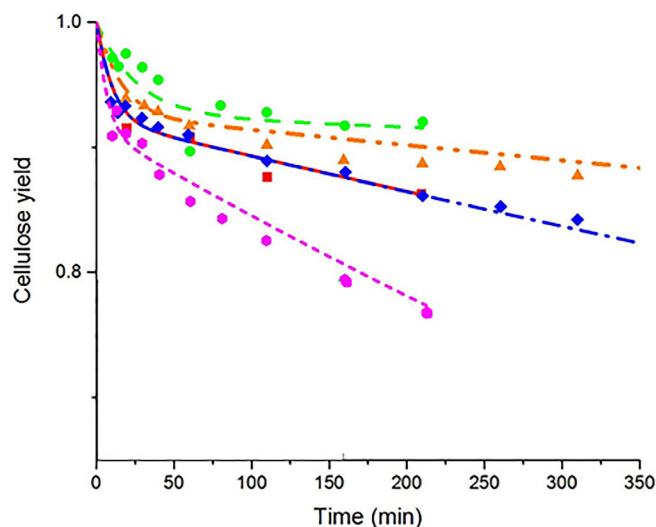
FIGURE 5 Cellulose degradation at [HO⁻] = 1.55 M, [HS⁻] = 0.31 M. Experimental data points[32] represented by symbols, simulation results expressed by lines. ■, —: 150°C, [Cl⁻] = 0 M; ●, -- -- --: 130°C, [Cl⁻] = 0.14 M; ▲, - .. - .. -: 140°C, [Cl⁻] = 0.14 M; ♦, - . - . -: 150°C, [Cl⁻] = 0.14 M; ●, - - - -: 160°C, [Cl⁻] = 0.14 M [Color figure can be viewed at wileyonlinelibrary.com]

hydrocellulose[38] and cellulose,[49] respectively. Alkaline hydrolysis activation energy for cellulose has been published to be 150.3 kJ/mol[50]. All reaction kinetic parameters were fitted with Kinfit software[34] for the most precise values. As it is visible from the Table 4 obtained results from the fitting are in line with published experimental values. The list of all cellulose reactions included in the model, their stoichiometries and reaction parameters are presented in Table 4.

Cellulose peeling reactions lead to consumption of alkali and yield loss. Figure 5 presents the results for the cellulose degradation process. As can be seen from this figure, the simulation fitted the experimental data accurately.

According to all the present results current model shows a good confidence between the simulation and experimental results. Obtained from Kinfit fitted kinetic parameters are in good line with published values. It shows that this approach offers an exceptional opportunity to examine the validity of various theories or hypothesis and provides deep knowledge based on reaction mechanisms and kinetic parameters of carbohydrate chemistry in pulping processes. The present modeling concept could be extended.

4 | CONCLUSIONS

In this paper, a detailed phenomenon-based model of carbohydrate reactions in kraft pulping was introduced. In this approach, the real chemistry and other essential phenomena of carbohydrate reactions, taking place in kraft pulping, is implemented in the model at molecular level. We have developed model that can predict carbohydrate degradation with good correlation to the experimental data. Moreover, obtained through fitting kinetic parameters are in line with published in literature, it proves that model can be used as tool for deep knowledge on reaction stoichiometry and kinetic parameters. However, due to the lack of experimental data, only simulations of kraft pulping with pine wood meal were used. It would be beneficial for the research to run simulation also with other wood species and check the accuracy of the model. However, already at this stage, the model can be used for modeling raw material fractionation into main wood components, and it could be very useful simulation tool for biorefinery cases,

especially if current, kraft pulping, part will be combined with previously developed models (hot-water extractions, bleaching, delignification). This approach offers an exceptional opportunity to examine different theories and hypothesis on reactions mechanisms as for existing process as for new chemistry processes, by including new compounds and reaction chemistries to database and simulator.

ACKNOWLEDGMENTS

NOTATION

A	frequency factor (depends on the rate equation)
COMA	comanic acid
CR	cellulose reducing end-groups
CNR	cellulose nonreducing end-group
CM	cellulose units in the middle chain
E_a	activation energy (J mol^{-1})
FSP	fiber saturation point (kg water[kg o.d.wood]$^{-1}$)
GGM	galactoglucomannan
GGMR	galactoglucomannan with a reducing end-group
GGMNR	galactoglucomannan with a nonreducing end-group
GGMM	galactoglucomannan units in the middle of the chain
HexA	hexenuronic acid
k	reaction rate constant (stoichiometry dependent units)
K	equilibrium constant (stoichiometry dependent units)
MeGlc	methylglucuronic acids
pK_a	acid dissociation constant
SSE	sum of squared errors of prediction
t	time (s)
T	temperature (K)
XYL	xylan
XYLR	xylan reducing end-group
XYLNR	xylan with nonreducing end-group
XYLM	middle group in xylan chain
XyloIsoSaccA	xyloisosaccharinic acid
XyloMetaSaccA	xylometasaccharinic acid

ORCID

Olesya Fearon https://orcid.org/0000-0003-0826-0475

REFERENCES

1. Sixta H, Potthast A, Krotschek AW. Chemical pulping process. In: Sixta H, ed. *Handbook of pulp*. Weinheim: WILEY-VCH Verlag GmbH & Co; 2006:109-229.
2. Sjöström E. *Textbook of wood chemistry: fundamentals and applications*. 2nd ed.San Diego: Academic Press, Inc.; 1993.
3. Chiang VL, Cho H, Puumala R, Eckert R, Fuller W. Alkali consumption in kraft pulping of Douglas-fir, western hemlock and red alder. *Tappi J*. 1987;70:101-104.
4. Vuorinen T, Fagerström P, Buchert J, Tenkanen M, Teleman A. Selective hydrolysis of hexenuronic acid groups and its application in ECF and TCF bleaching of kraft pulps. *J Pulp Paper Sci*. 1999;25(5):155-162.
5. Clayton DW. The alkaline degradation of some hardwood 4-O-methyl-d glucuronoxylan. *Svensk Papperstidning*. 1993;66(4):115-119.
6. Vroom KE. The H-factor: a means of expressing cooking times and temperatures as a single variable. *Pulp Pap Mag Can*. 1957;58:228-231.
7. Kleinert TN. Mechanism of alkaline delignification. I. the overall reaction patern. *Tappi J*. 1966;49(2):53-57.
8. Hatton JV. Development of yield prediction equations in kraft pulping. *Tappi J*. 1973;56:97.
9. LeMon S, Teder A. Kinetics of the delignification in kraft pulping. *Svensk Papperstidning*. 1973;76(11):228-233.
10. Smith CC, Williams TJ. Mathematical modeling, simulation and control of the operation of a kamyr continuous digester for the kraft process [Ph.D. Thesis]. West Lafayette: Purdue University; 1974.
11. Christensen T, Albright LF, Williams TJ. A kinetic mathematical model for the kraft pulping of wood. *Tappi Annual Meet*. 1983;239-243.
12. Gustafson RR, Slelcher CA, McKean WT, Finlayson BA. Theoretical model of the kraft pulping process. *Ind Eng Chem Process Des*. 1983;22(1):87-96.
13. Pu Q, Sarkanen K. Donnan equilibria in wood-alkali interactions. Part 2 effect of polysaccharide ionization at high alkalinities. *J Wood Chem Technol*. 1991;11(1):1-22.
14. Gustavson CA, Al-Dajani WW. The influence of cooking conditions on the degradation of hexenuronic acid, xylan, glukomannan and cellulose during kraft pulping of softwood. *Nord Pulp Paper Res J*. 2000;15(2):160-167.
15. Andersson N, Wilson DI, Germgård U. An improved kinetic model structure for softwood kraft pulping. *Nord Pulp Paper Res J*. 2003;18(2):200-209.
16. Johansson D, Germgård U. Carbohydrate degradation during softwood kraft cooking – influence on cellulose viscosity, carbohydrate composition and hexenuronic acid content. *Nord Pulp Paper Res J*. 2008;23(3):292-298.
17. Wigell A, Brelid H, Theliander H. Kinetic modelling of (galacto) glucomannan degradation during alkaline cooking of softwood. *Nord Pulp Paper Res J*. 2007;22(4):495-499.
18. Nieminen K, Paananen M, Sixta H. Kinetic model for carbohydrate degradation and dissolution during kraft pulping. *Ind Eng Chem Res*. 2014;53:11292-11302.
19. Whistler RL, BeMiller JN. Alkaline degradation of polysaccharides. *Adv Carbohydr Chem*. 1958;13:289-329.
20. Aurell R, Hartler N. Kraft pulping of pine. II. Influence of the charge of alkalio on the yield, carbohydrate composition, and properties of the pulp. *Svensk Papperstidn*. 1965;68:97-102.
21. Knill CJ, Kennedy JF. Degradation of cellulose under alkaline conditions. *Carbohydr Polym*. 2003;51(3):281-300.
22. Norimoto M. Chemical modification of wood. In: Hon DN, Shiraishi N, eds. *Wood and cellulosic chemistry*. 2nd ed.New York: Marcel Dekker Inc.; 2001:573-621.
23. Bogren J, Brelid H, Theliander H. Towards a general kraft delignification model. *Nord Pulp Paper Res J*. 2009;24(1):33-37.
24. Wisnewski PA, Doyle FJI, Kayihan F. Fundamental continuous-pulp-digester model for simulation and control. *AIChE J*. 1997;43(12):3175-3192.
25. Bhartiya S, Dufour P, Doyle FJ. Fundamental thermal-hydraulic pulp digester model with grade transition. *AIChE J*. 2003;49(2):411-425.

26. Miyanishi T, Shimada H. Improvement of pulp strength and yield by computer simulation on lo-solids kraft cooking. *Tappi J*. 2001;84 (6):65.

27. Choi H, Kwon JS. Multiscale modeling and control of kappa number and porosity in a batch pulp digester. *AIChE J*. 2019;65(6):e16589.

28. Choi H, Kwon JS. Modeling and control of cell wall thickness in batch delignification. *Comp Chem Eng*. 2019;128:512-523.

29. Kuitunen S, Vuorinen T, Alopaeus V. The role of donnan effect in kraft liqour impregnation and hot water extraction. *Holzforschung*. 2013;67:511-521.

30. Fearon O, Kuitunen S, Ruuttunen K, Alopaeus V, Vuorinen T. Detailed modeling of kraft pulping chemistry: Delignification. *to be published*; 2020.

31. Paananen M, Tamminen T, Nieminen K, Sixta H. Galactoglucomannan stabilization during the initial kraft cooking of scots pine. *Holzforschung*. 2010;64(6):683-692.

32. Paananen M, Liitiä T, Sixta H. Further insight into carbohydrate degradation and dissolution behavior during kraft cooking under elevated alkalinity without and in the presence of anthraquinone. *Ind Eng Chem Res*. 2013;52:12777-12784.

33. Bogren J, Brelid H, Theliander H. Reactions kinetics of softwood kraft delignification - general considerations and experimental data. *Nord Pulp Paper Res J*. 2007;22(2):177-183.

34. Jakobsson K, Aittamaa J. Kinfit parameter optimization software. http://chemtech.aalto.fi/en/research/groups/chemical_engineering/ software/kinfit/. Accessed September 29, 2019.

35. Lehto JH. Characterization of mechanical and chemical pulp fibers. 58th Appita Annual Conference And Exhibition; Canberra, ACT, Australia; 19–21 April 2004, Paper 3A13, 8 p.

36. Fernandez EC.Douglas-fir bark: Structure and alkaline degradation of a glucomannan. [Ph.D. Thesis]. Oregon State University; 1977.

37. Pennings AJ, Prins W. The polyelectronic nature of cellulose gels in alkaline solutions. *J Polym Sci*. 1962;58:229-248.

38. Christensen JJ, Rytting JH, Izatt RM. Thermodynamics of proton dissociation in dilute aqueous solutions. Part XV. Proton dissociation from several monosaccharides at 10 and 40 C. *J Chem Soc B: Phys Org*. 1970;1946-1948.

39. Young RA, Liss L. A kinetic study of the alkaline endwise degradation of gluco- and galactomannans. *Cell Chem Technol*. 1978;12:399-411.

40. Lai YZ. Kinetic evidence of anionic intermediated in the base-catalyzed cleavage of glycosidic bonds in the methyl D-glucopyranosides. *Carbohydr Res*. 1972;24:57-65.

41. Chen CH.Douglas-fir bark: isolation and characterization of a hollocellulose fraction [PhD. thesis]. Oregon State University; 1973.

42. Johansson MH, Samuelson O. Alkaline destructuin of birch xylan in the light of recent investigations of its structure. *Svensk Papperstidning*. 1977;80(16):519-524.

43. Kohn R, Kovak P. Dissociation constants of D-galacturonic and D-glucuronic acid and their O-methyl derivatives. *Chem Pap*. 1978;32 (4):478-485.

44. Bogren J, Brelid H, Theliander H. Effect of pulping conditions on the rates of formation and degradation of hexenuroic acid in scots pine. *J Pulp Paper Sci*. 2008;34(1):23-29.

45. Bogren J, Brelid H, Theliander H. Assessment of reaction kinetic models describing delignification fitted to well-defined kraft cooking data. *Nord Pulp Paper Res J*. 2008;23(2):210-217.

46. Nieminen K, Testova L, Paananen M, Sixta H. Novel insight in carbohydrate degradation during alkaline treatment. *Holzforschung*. 2015; 69(6):667-675.

47. Chai X, Yoon S, Zhu JY, Li J. The fate of hexenuroic acid groups during alkaline pulping of loblolly pine. *J Pulp Paper Sci*. 2001;27(12): 403-406.

48. Haas DW, Hrutfiord BF, Sarkanen KV. Kinetic study on the alkaline degradation of cotton hydrocellulose. *J Appl Polym Sci*. 1967;11: 587-600.

49. Van Loon LR, Glaus MA. Review of the kinetics of alkaline degradation of cellulose in view of its relevance for safety assessment of radioactive waste repositories. *J Environ Polym Degrad*. 1977;5(2): 97-109.

50. Lai YZ, Sarkanen KV. Kinetics of alkaline hydrolysis of glycosidic bonds in cotton cellulose. *Cell Chem Technol*. 1967;1(5):517-527.

51. Guan QQ, Zhou HJ, Peng LC, et al. Mathematical model for predicting the dissolution behaviors of hemicelluloses during cold caustic extraction process. *AIChE Lett: Biomol Eng Bioeng Biochem Biofuels Food*. 2019;65(1):13-17.